Airborne Imaging System Using a Cryogenic 90-GHz Receiver

BERND VOWINKEL, JUHANI K. PELTONEN, WERNER REINERT, KONRAD GRÜNER, AND BERND AUMILLER

Abstract—**A cryogenic 90-GHz receiver has been developed with a noise figure of 2.36 dB ((double sideband) (DSB)) and an instantaneous bandwidth of 1.2 GHz. The cooled front-end consists of a Schottky-barrier mixer followed by a GaAs FET IF amplifier. The radiometer is small in size and weighs only 52 kg, including the refrigerator system. It is part of an airborne imaging system, that has been flight-tested aboard a Dornier Do 28 aircraft. First test results are presented.**

I. Introduction

AIRBORNE MILLIMETER-WAVE imaging systems are of great practical interest for the remote sensing of the environment. In particular the frequency region around 90 GHz is very useful, because a high angular resolution can be achieved with small antennas and at the same time contrast losses due to weather conditions are still small. Airborne systems to date have yielded excellent results [1]–[3] but have also shown that a further reduction in the receiver noise temperature is necessary.

The improvements in solid-state millimeter-wave devices and GaAs FET's in the last years and the availability of small size closed cycle refrigerators have made it possible to develop a cryogenic radiometer with a state-of-the-art temperature resolution and relatively light weight. The system has been flight-tested aboard a Dornier Do 28 aircraft. Images of the ground have been made from various altitudes with 1° angular resolution.

II. Basic Concept

The imaging system consists of an oscillating parabolic mirror, a cryogenic radiometer, and digital data processor (see Fig. 1). The data are recorded on magnetic tape for further analysis on the ground and also displayed on a screen for quick-look evaluation. The minor axis diameter of the mirror is 200 mm, giving an angular resolution of about 1°. For absolute temperature calibration, a rotating absorber is placed between the mirror and radiometer input. The absorber paddle is synchronized with the mirror such that it covers the radiometer input, when the mirror changes the direction of movement. The maximum oscillation frequency of the mirror is 35 Hz and the total scan angle is 30°.

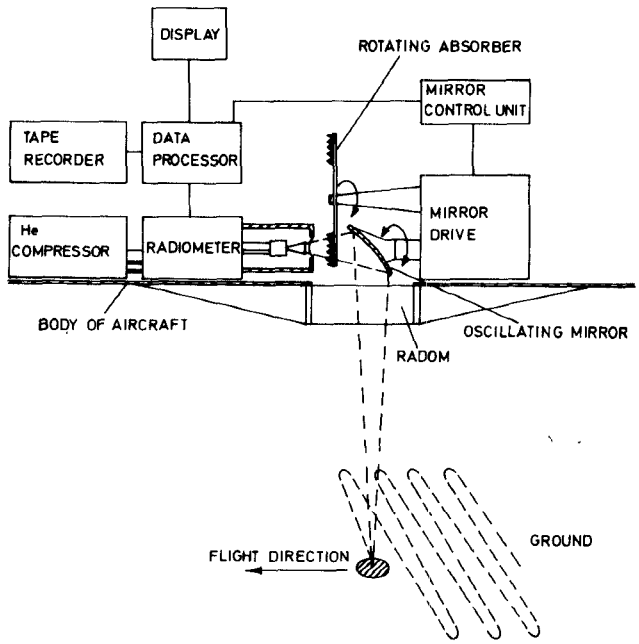

Fig. 1. Sketch of the principal configuration.

The radiometer is a total power system, consisting of a cryogenic GaAs Schottky-barrier mixer with built-in GaAs FET IF amplifier and an uncooled IF postamplifier with high gain. The mixer is driven by a GaAs Gunn oscillator. Fig. 2 shows a block diagram of the front end. The cooled components are located in a vacuum chamber in order to prevent convection and condensation of the air. A 50-μ thick Mylar window is inserted in front of the horn antenna, that has negligible insertion losses at millimeter wavelengths.

Mixer and FET preamplifier are cooled to 20 K using a closed cycle refrigerator (Cryogenic Tech. Inc. Model 21 SC). The two-stage expander module is integrated into the radiometer assembly and is connected to the compressor by two flexible helium pipes. The power consumption of the compressor is 1.1 kW and the weight is 39 kg. The

Manuscript received May 13, 1980; revised January 5, 1981. A condensed version of this paper has been presented at the 1980 IEEE-MTTS International Microwave Symposium, Washington, DC.

B. Vowinkel is with Radioastronomisches Institut der Universität Bonn, Auf dem Huegel 71, D-5300 Bonn, Federal Republic of Germany.

J. K. Peltonen is with Radioastronomisches Institut der Universität Bonn, Auf dem Huegel 71, D-5300 Bonn, Federal Republic of Germany, on leave from Helsinki University of Technology, Helsinki, Finland.

W. Reinert is with Radioastronomisches Institut der Universität Bonn, Auf dem Huegel 71, D-5300 Bonn, Federal Republic of Germany.

K. Grüner and B. Aumiller are with DFVLR, Institut fuer HF-Technik, D-8031 Oberpfaffenhofen, Federal Republic of Germany.

0018-9480/81/0600-0535$00.75 ©1981 IEEE

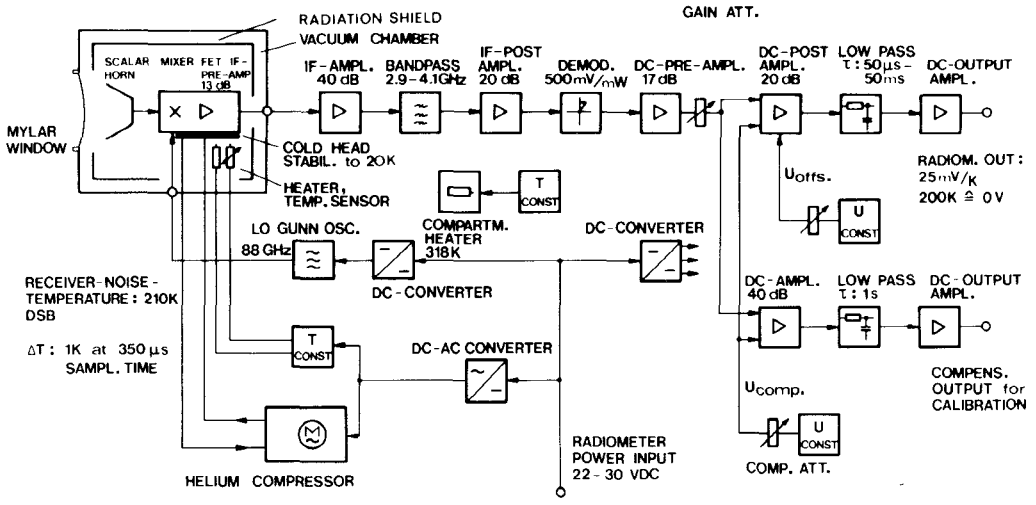

Fig. 2. Block diagram of the radiometer.

weight of the radiometer is 13 kg (including expander module).

III. Local Oscillator

The local oscillator is a GaAs Gunn diode mounted in a full height WR-12 waveguide [4]. A radial disk with a diameter of about $\lambda/2$ determines the frequency of oscillation. The disk diameter was reduced iteratively until the correct frequency was attained. In order to prevent mechanical sensitivity, no tuning elements are used. Also the backshort is fixed at a distance of about $\lambda_g/4$ to the center of the resonator. The optimum distance for each diode was found experimentally in a test oscillator with adjustable backshort.

The maximum output power that has been achieved was 30 mW at 88 GHz using the second harmonic oscillation of an Alpha Industries 44-GHz diode. For the radiometer an oscillator of lower output power was used, because the power requirement for the mixer was only about 1 mW.

IV. Mixer

The mixer is a broad-band version of a design presented at the 9th European Microwave Conference [5]. The LO is coupled via a TE_{111}-mode cavity filter into the signal waveguide, which is an electroformed transition to a reduced height (1/3) waveguide cross section. Due to the bandpass frequency response of the filter (see Fig. 3) the signals in both sidebands of the mixer are reflected at the filter. Therefore at the signal frequencies the filter acts as a backshort. The distance between filter and mixer diode was experimentally optimized for minimum noise figure. The filter consists of two parts that are glued together after electrochemical polishing of the surface, and resonance-frequency adjustment. For the adjustment, the length of the cavity was slightly reduced by grinding the cylinder wall. The material used for the cavity is Vacodil (Vacuumschmelze Hanau, Federal Republic of Germany), which has an extremely small temperature expansion coefficient. The insertion loss of the filter at LO frequency is 0.6 dB and more than 20 dB at the sidebands.

The GaAs Schottky-barrier diode was fabricated in our

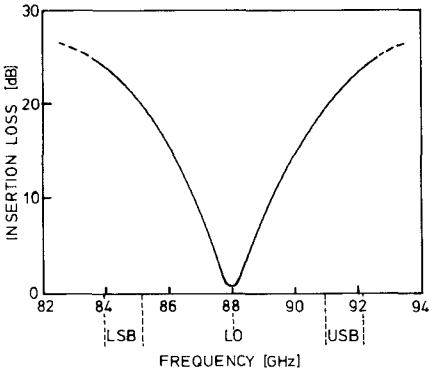

Fig. 3. Frequency response of LO filter.

laboratories by means of electron beam lithography, using commercially available substrate material (Plessey). The epilayer thickness of the material is 0.15 μm and the doping concentration is $2 \cdot 10^{16}$ cm^{-3}. The buffer layer doping cocentration is $4 \cdot 10^{18}$ cm^{-3}. The diameter of the Schottky contacts is 2.5 μm, giving a series resistance of 9 Ω and a diode ideality factor (characteristically inverse slope of $V-\log I$ curve) of 1.09.

The diode is soldered to a coaxial low-pass filter, that rejects the RF. A mixture of Araldite and quartzmeal was used to fix the choke. The measured conversion loss of the mixer is 5.8 dB and the SSB noise figure is 5.7 dB (790 K) at room temperature. At 20 K the SSB noise figure is reduced to 2.0 dB (170 K). These values are without the IF amplifier contribution, but including the losses of horn antenna, circular-rectangular waveguide transition, LO coupling circuit, and IF matching circuit (see Table I). The temperature dependence of the DSB mixer noise temperature is shown in Fig. 4.

The 3–4-GHz band was chosen for the IF. Optimum IF impedance levels ranging from 80 to 120 Ω were estimated for the Schottky-diode in a broad-band mixer. The IF impedance was matched to a 50-Ω line with two short sections of successively high- (air line) and low-impedance transmission lines. The high-impedance microstrip line also reduces mechanical stresses between the diode mount and

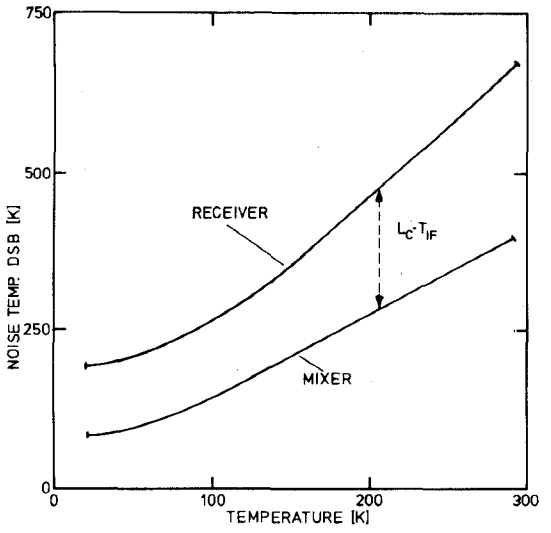

Fig. 4. Temperature dependence of DSB mixer noise temperature and DSB receiver noise temperature.

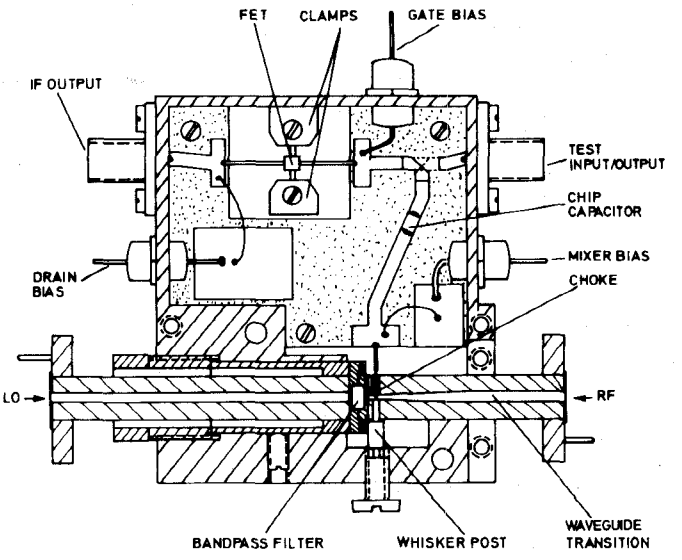

Fig. 5. Cross-sectional view of mixer/IF amplifier.

TABLE I
NOISE CONTRIBUTIONS OF RECEIVER COMPONENTS TO THE TOTAL RECEIVER NOISE TEMPERATURE

Device	Gain/Loss dB	Physical Temp. K	Noise Temp. K	Noise Contrib. to T_{rec} K
Mylar Window	~0	297	~0	~0
Horn Antenna	0.1	20	~0	5
circ.-rectang. Transition	0.2	20	~0	10
Mixer incl. LO coupling circ.	DSB 2.8	20	DSB 70	70
IF Matching Circuit	0.4	20	2	20
Cryog. FET	13	20	45	86
Postamplifier	40	297	200	19
total Receiver (double sideband)				210

TABLE II
RECEIVER AND IF NOISE TEMPERATURES FOR DIFFERENT INSTANTANEOUS BANDWIDTHS

IF (GHz)	T_{Rec} (DSB)	T_{IF}^{+}	$N_{\Delta T=1,\ \alpha=1}$
room temperature (293 K)			
3.3 - 3.9	670 K (5.2 dB)	140 K (1.7 dB)	709 sec^{-1}
2.9 - 4.1	710 K (5.4 dB)	160 K (1.9 dB)	1302 sec^{-1}
cooled (20 K)			
3.3 - 3.9	190 K (2.19 dB)	45 K (0.63 dB)	3099 sec^{-1}
2.9 - 4.1	210 K (2.36 dB)	55 K (0.75 dB)	5671 sec^{-1}
Test system with cryogenic parametric amplifier			
3.7 - 4.2	113 K (1.43 dB)	15 K (0.22 dB)	3795 sec^{-1}

+) not including postamplifier contribution

the matching circuit. The dielectric substrate material used for the low- and medium-impedance sections is RT Duroid D 5880.

V. CRYOGENIC GaAs FET AMPLIFIER

A single-stage cooled FET amplifier was developed for the 3–4-GHz IF band. A nominal transducer power gain of 12–13 dB was chosen to reduce the postamplifier contribution to the total IF noise temperature to about 10 K and to maintain amplifier stability at cryogenic temperatures. The transistors NE 24483, NE 38883 (Nippon Electric Company), and MGF 1402 (Mitsubishi) have been tested. Best results at cryogenic temperatures were achieved with the transistor MGF 1402. The results for different bandwidths are listed in Table II.

For the input and output matching networks, double-section matching transformers in microstrip technology have been chosen. In order to achieve a broad matching bandwidth, which requires short (less than 0.1 λ) matching elements, the impedance ratio between the high- and low-impedance elements has to be high. Because high-impedance sections above 120 Ω are hard to realize in normal microstrip technology, air lines with increased distance (2 mm) to the ground plane were used to achieve an impedance of 200 Ω. The gate and drain leads of the packaged transistor were used as conductors for the high-impedance sections. The solder connections were made with indium, to avoid cracking at cryogenic temperatures. The transistor is fixed by two clamps that can be moved somewhat apart from the transistor in order to increase the inductive feedback, caused by the inductance of the transistor source leads. The main effects of the feedback are a reduction of the gain and a reduction of the magnitude of S_{11} [6]. The latter gives a broader input matching bandwidth and a better input VSWR. A suitable compromise between gain reduction and matching bandwidth was achieved with a 2-mm source lead length.

The FET amplifier was integrated with the mixer mount in a common housing (see Fig. 5). A 50-Ω test port was added to facilitate separate testing of the mixer and amplifier. The length of the 50-Ω line was selected to compensate the residual mismatches between the mixer IF output and the transistor at the band edges. Thus a cryogenic isolator was not absolutely necessary between the two circuits.

VI. Performance of the Radiometer

The performance of a radiometer, that is part of an imaging system, can be expressed by the data rate (number of samples per second) which is available for a temperature resolution of 1 K. Knowing the effective instantaneous bandwidth and the noise temperature of the radiometer, the data rate can be calculated with

$$N_{\Delta T=1K} = \frac{B}{\alpha^2 (T_A + T_{\text{rec}})^2}$$

where

- B effective instantaneous bandwidth, in hertz,
- T_{rec} receiver noise temperature, in degrees Kelvin,
- T_A antenna noise temperature, in degrees Kelvin, and
- α constant depending on the type of receiver (e.g., Dicke system) α is ≥ 1.

In airborne radiometry, the antenna noise temperature T_A varies between about 290 K for forests and about 180 K for water surfaces. For metal surfaces (vehicles) antenna temperatures below 100 K are possible. For the calculation of the medium available data rate a value of $T_A = 250$ K may be assumed. In order to find the optimum IF bandwidth (for highest data rate) the total receiver noise temperature versus the IF has been measured with a tunable narrow-band (60 MHz) IF filter (see Fig. 6). For broad-band measurements two bandpass filters were available, one ranging from 3.3 to 3.9 GHz and the other one from 2.9 to 4.1 GHz. The results clearly show that up to an instantaneous bandwidth of 1.2 GHz the integral receiver noise temperature increases very slowly, but rather rapidly above that band, so that the band ranging from 2.9 to 4.1 GHz is close to the optimum. Of course, these results depend mainly on the matching networks between mixer and FET and also on the inductive feedback of the transistor.

For test measurements the mixer has been mounted in a receiver system with a cryogenic parametric IF amplifier (AIL model 4500-1). The result in this configuration was 113 K (DSB) for the total receiver noise temperature, which is considered one of the best values that have been reached up to now in this frequency region. But owing to the small bandwidth of the parametric amplifier, the available data rate is still less than the value for the broad-band system with considerably higher noise temperature (see Table II). Therefore the broad-band system with FET IF amplifier was chosen for the final version.

A further advantage of this system is the smaller size, which made it possible to use a smaller refrigeration system (CTI 21 instead of CTI 350) and also the stability of the cryogenic FET amplifier is better compared to the parametric amplifier. The short term stability of the total receiver system (at constant temperature) is better than 0.005 dB/min and the long term stability is better than 0.02 dB/h.

Table I shows the noise temperature contributions of the receiver elements to the total receiver noise temperature for the broad-band system. The IF noise temperatures were measured with an AIL hot/cold body (type 70). The

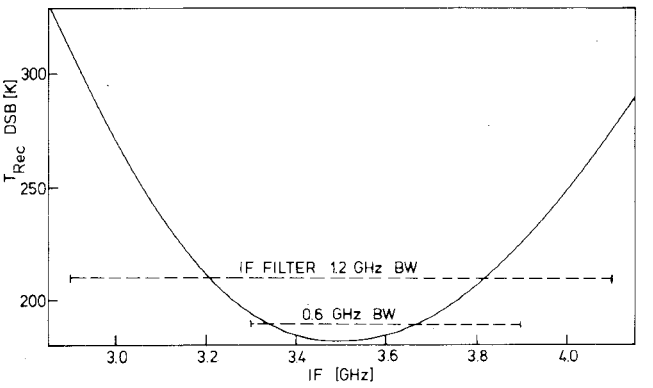

Fig. 6. DSB receiver noise temperature versus IF.

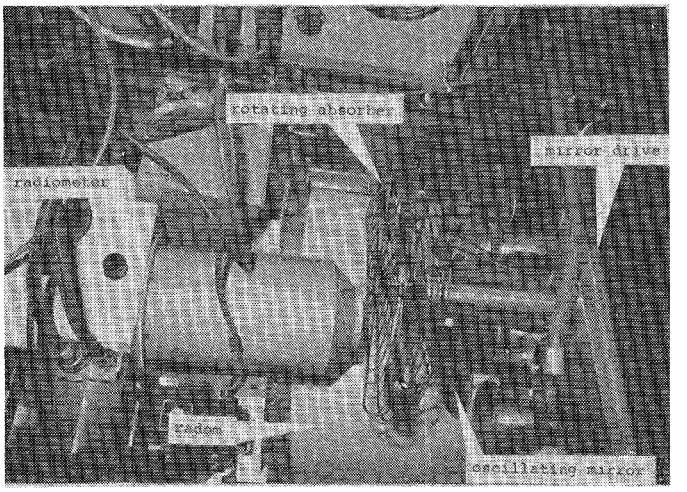

Fig. 7. Photograph of radiometer and mirror drive system, mounted to the body of the aircraft.

double-sideband receiver noise temperature has also been measured by hot/cold method, using absorber material, at room temperature and at liquid nitrogen temperature, that is successively placed in front of the horn antenna. The accuracy of this method is considered to be better than ± 10 K for the resulting receiver noise temperature.

In fall 1980 the IF-part of the front end has been redesigned using the improved transistor MGF 1412 (Mitsubishi) [7]. With increased inductive feedback of the transistor circuit, the instantaneous bandwidth has been improved to 2.4 GHz (1.6–4.0 GHz), whereas the total receiver noise temperature remained at about the same value as stated in Table II for the broad-band version.

A. First Results

In February 1980 first flight tests of the system were made aboard a Dornier Do 28 aircraft. Fig. 7 shows the radiometer and the mirror drive system, mounted to the body of the aircraft. The strong vibrations caused by the engines did not effect the quality of the radiometer output. Until December 1980 about 10 flights with the system have been performed and the cooled components have been temperature cycled about 30 times, without any degradation of the performance.

Figs. 8–12 are photographs taken from a quick-look presentation on a color-screen. In order to show the quality

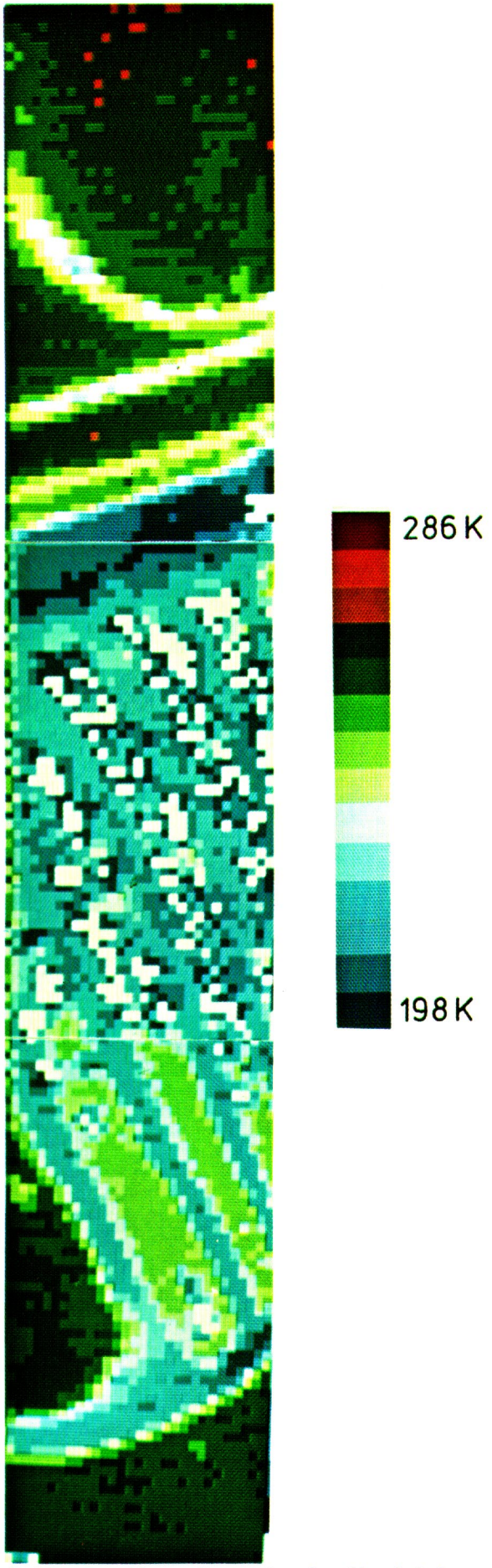

Fig. 8. Parking area with cars; linear colorscale; white pixels for temperatures less than 198 K (metal objects). Image area: is 43 by 250 m.

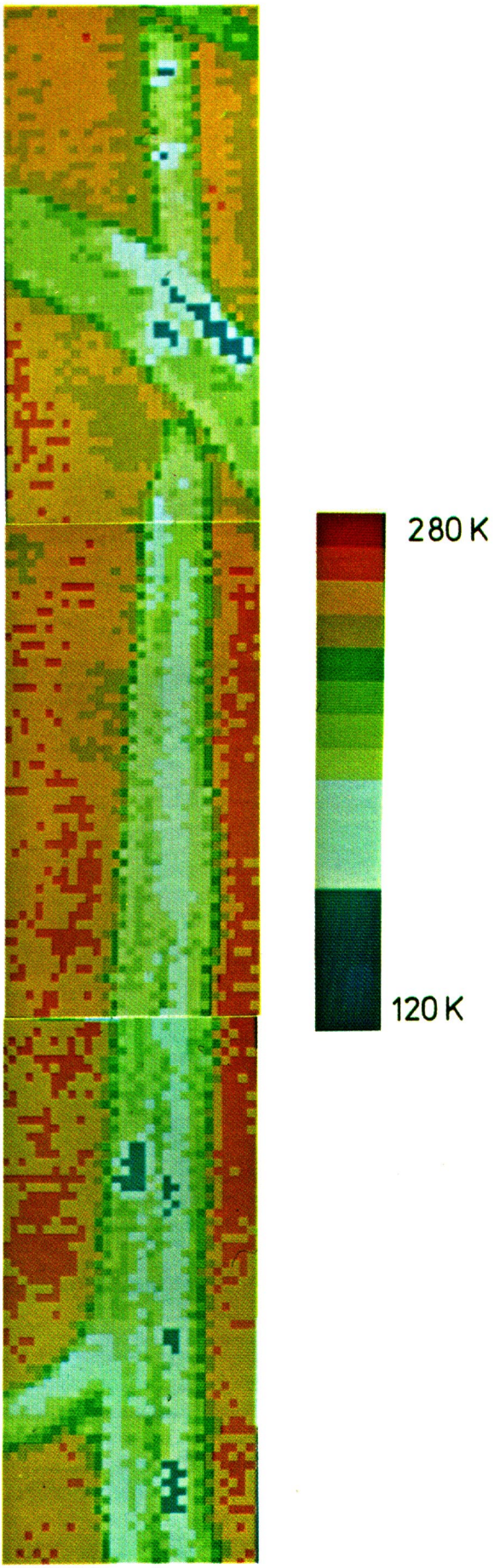

Fig. 9. Passenger cars and trucks on a highway; nonlinear colorscale. The image area of 43 by 250 m was scanned within 5 s.

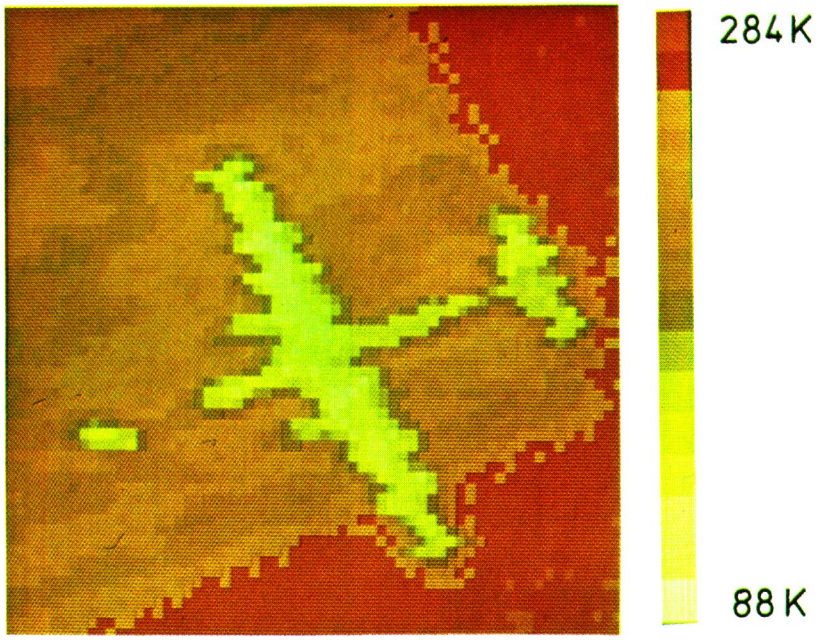

Fig. 10. Image of a parked twin-engine aircraft on a concrete platform. The image area of 45 by 45 m was scanned within 1 s.

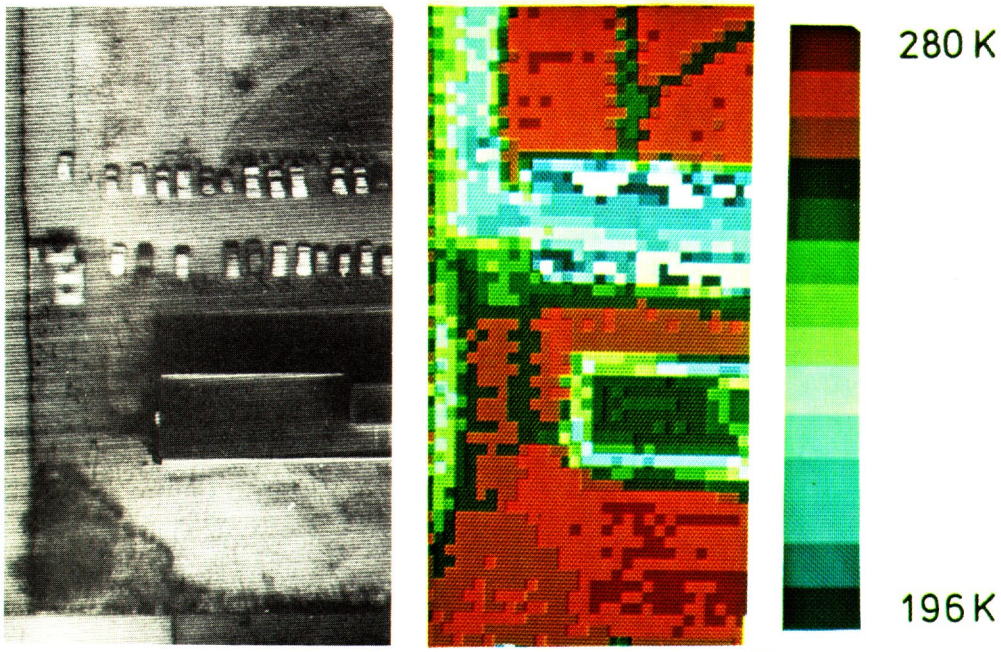

Fig. 11. Building with parking area and cars. Infrared image of the same area at the left side. The images were obtained from an altitude of 85 m at an aircraft speed of 50 m/s. The shown area is 43 by 85 m. Luftbildfreigabe: Regierung von Oberbayern, GS 328/256.

of the radiometer output signal, no special image processing was done. Only a color coding was used, to improve the contrast. The given temperatures are antenna noise temperatures. Although there have been some problems during the first flight tests with powerline filtering, which caused signal errors and by that way somewhat blurred contours, the first results are excellent. Most of the flights were carried out at an altitude of 85 m (280 ft) above ground (Figs. 8–11), which results in a spatial resolution better than 1.6 m. In this case a scan frequency of 35 Hz is necessary for an overlap of 50 percent for two successive lines and an aircraft speed of 50 m/s.

Fig. 8 shows a parking area, half of which is occupied by passenger cars (white pixels). Access and exit roads as well as parking areas are distinctly separated from grassy areas. To map the terrain shown, 5 s were needed, which corresponds to a length of about 250 m. For this image only one scan direction was processed. Fig. 9 shows a highway with cars and trucks on it (blue pixels). Another road crosses the highway by a bridge. At one side of the bridge there is

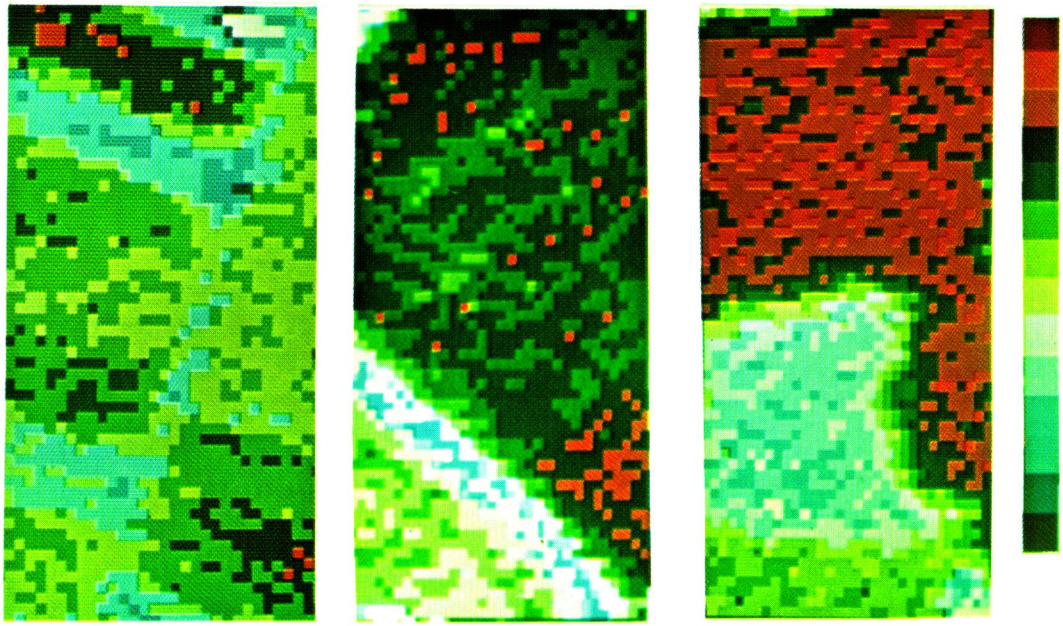

(a) (b) (c)

Fig. 12. Different kinds of vegetation; altitude 400 m; linear colorscale. (a) Different types of fields; temperature window 243 K–263 K; 1.5 K per colorstep. (b) Forest (dark green), fields (light green); temperature window 244 K–272 K. (c) Forest (brown), meadow partly covered with snow (blue); temperature window 238 K–266 K.

footpath made of metal (white and blue pixels). The areas around the roads are mainly covered by grass (yellow and red) and bushes (light green). Fig. 10 shows a parked twin-engine aircraft on a concrete platform, surrounded by meadows. A small vehicle is parked in front of the aircraft. Only 1 s was needed to obtain this image (both scan directions were processed). Fig. 11 shows a building with parking area. An infrared reference image (10 μm) of the same area is given on the left side for comparison. Most of the details in the infrared image can also be identified in the 90-GHz image, although the spatial resolution is considerably lower. The three images in Fig. 12 were taken from an altitude of 400 m (1300 ft) with a scan frequency of 7 Hz. Areas with different vegetation were overflown, to study the temperature resolution of the system. Fig. 12(a) indicates that a temperature resolution of about 1 K is obtained, which is somewhat worse than the expected theoretical value. It was found that this degradation was caused by the above mentioned powerline problem. This is also an explanation for the Moire pattern in Fig. 12(c). After the first tests, the powerline problem was settled and the latest results are in agreement with the theoretical expected temperature resolution.

VII. Conclusion

A cryogenic 90-GHz receiver has been developed which has, to the knowledge of the authors, the highest resolution at present for radiometry in this frequency region. This has been achieved by using state-of-the-art millimeter-wave diodes, a cryogenic FET amplifier, and a high-speed scanning antenna. The radiometer has been used for airborne radiometry aboard a small aircraft. First flight tests have shown that the system is reliable and easy to operate.

For an improved resolution, a further reduction of the receiver noise temperature is of very limited value, because the contribution to the total system noise temperature ($T_{\text{rec}} + T_A$) is at present only about 50 percent. Even a noise-free receiver would lead to an improvement in the data rate of only factor 4 compared to the presented receiver. The only way to increase the resolution by orders of magnitude is now the development of multichannel receivers and a further increase of the instantaneous bandwidth.

Acknowledgment

The authors wish to thank E. Becker of the University of Bonn for the mechanical construction of the radiometer front end and G. Kahlisch, J. Oberberger, G. Griebel, A. Grossman, and H. Schreiber of the DFVLR for the mechanical construction of the mirror drive, the antenna reflector, the integration of the angle decoder, and the installation and operation of the test system.

References

[1] J. P. Hollinger, J. E. Kenney, and B. E. Troy, "A versatile millimeter wave imaging system," *IEEE Trans. Microwave Theory Tech.*, vol. MTT-24, pp. 786–793, Nov. 1976.

[2] K. Gruener and B. Aumiller, "Mikrowellenradiometrie des Erdbodens," *Mikrowellen Magazin*, vol. 5/79, pp. 289–293.

[3] K. Gruener, "Advances in the Field of Microwave Radiometry," in *Proc. 8th European Microwave Conf.*, 1978, pp. 3–4.

[4] J. Ondria, "Wide-band mechanically tunable *W*-band CW Gunn diode oscillators," in *Proc. AGARD Conf.*, 1978, pp. 12–1, 12–15.

[5] B. Vowinkel, "Image recovery millimeter-wave mixer," in *Proc. 9th European Microwave Conf.*, 1979, pp. 726–730.

[6] D. Burns, "The 600-MHz noise performance of GaAs MESFET's at room temperature and below," NRAO Internal Rep. No. 197.

[7] B. Vowinkel, "Cryogenic 2–4 GHz FET Amplifier," *Electron. Lett.*, vol. 16, no. 19, pp. 730–731, Sept. 1980.